Biocatalysis, Protein Engineering, and Nanobiotechnology **Biotechnology and Bioengineering**
DOI 10.1002/bit.25592

Coupling limonene formation and oxyfunctionalization by mixed-culture resting cell fermentation†

Christian Willrodt[1,2], Anna Hoschek[1], Bruno Bühler[1], Andreas Schmid[2*], and Mattijs K. Julsing[1]

Running Title: De novo synthesis of perillyl acetate

[1] Laboratory of Chemical Biotechnology, Department of Biochemical and Chemical Engineering, TU Dortmund University, Dortmund, Germany
[2] Department Solar Materials, Helmholtz Centre for Environmental Research (UFZ), Leipzig, Germany

*Correspondence to:
Andreas Schmid
Department Solar Materials, Helmholtz Centre for Environmental Research (UFZ), Permoserstrasse 15, 04318 Leipzig, Germany
telephone: +0049-341-235-1246
fax: +0049-341-23545-1286
email: andreas.schmid@ufz.de

†This article has been accepted for publication and undergone full peer review but has not been through the copyediting, typesetting, pagination and proofreading process, which may lead to differences between this version and the Version of Record. Please cite this article as doi: [10.1002/bit.25592]

Additional Supporting Information may be found in the online version of this article.

Received December 18, 2014; Revision Received February 13, 2015; Accepted March 10, 2015

Abstract

Metabolic engineering strategies mark a milestone for the fermentative production of bulk and fine chemicals. Yet, toxic products and volatile reaction intermediates with low solubilities remain challenging. Prominent examples are artificial multistep pathways like the production of perillyl acetate (POHAc) from glucose via limonene. For POHAc, these limitations can be overcome by mixed-culture fermentations. A limonene biosynthesis pathway and cytochrome P450 153A6 (CYP153A6) as regioselective hydroxylase are used in two distinct recombinant *E. coli*. POHAc formation from glucose in one recombinant cell was hindered by ineffective coupling of limonene synthesis and low rates of oxyfunctionalization. The optimization of P450 gene expression led to the formation of 6.20 ± 0.06 mg g_{cdw}^{-1} POHAc in a biphasic batch cultivation with glucose as sole carbon and energy source. Increasing the spatial proximity between limonene synthase and CYP153A6 by a genetic fusion of both enzymes changed the molar limonene/POHAc ratio from 3.2 to 1.6. Spatial separation of limonene biosynthesis from its oxyfunctionalization improved POHAc concentration 3.3-fold to 21.7 mg L^{-1} as compared to a biphasic fermentation. Mixed-cultures of *E. coli* BL21 DE3 containing the limonene biosynthesis pathway and *E. coli* MG1655 harboring either CYP153A6, or alternatively a cymene monooxygenase, showed POHAc formation rates of 0.06 or 0.11 U g_{cdw}^{-1}, respectively. This concept provides a novel framework for fermentative syntheses involving toxic, volatile, or barely soluble compounds or pathway intermediates.

Keywords: industrial biotechnology, fermentation, oxygenated monoterpenoids, limonene, cytochrome P450, metabolic and reaction engineering

Introduction

Products and intermediates of central carbon metabolism are of limited structural complexity, hydrophilic and charged (http://www.ecocyc.org). The largest part of industrially relevant natural products, however, is structurally complex, hydrophobic, volatile, and not charged (Liese et al. 2006). Which concepts were evolved in nature to cope with these properties? Prominent examples are the modular polyketide synthases, assembling complex chemical structures by intermediate channeling through different subunits (Staunton and Weissman 2001), and the synthesis, production, and storage of volatiles in specialized plant cells or tissues containing designated cavities, ducts or vacuoles, or in organelles (Pichersky et al. 2006).

Specialized organisms and their parts like e.g. plant cells, are seldom of industrial use as they are typically characterized by slow growth, fastidious nutrient requirements, and limited scalability (Zhang et al. 2011). Alternatively, recombinant microbial strains are applied, although their genetic repertoire and subcellular architecture are not optimized by evolution for natural product synthesis. The development of biotechnological production traditionally focuses on gene-based metabolic engineering strategies importing and synchronizing foreign genetic elements like genes or promotors.

Successful implementations of biotechnological processes however, necessitate the concerted optimization of genetic, metabolic, reaction, and process related parameters, taking into account the properties of the intermediates and products of a given pathway. The biotechnological production of monoterpenoids, such as perillyl acetate or perillyl alcohol can serve as a model system for new process design concepts meeting these requirements. These compounds are of great interest for the cosmetic, food, and pharmaceutical industries due to their olfactory, antimicrobial, and anticarcinogenic properties (Schewe et al. 2011; van der Werf et al. 1997).

The de novo formation of monoterpenes in general using engineered *E. coli* (Alonso-Gutierrez et al. 2013; Sarria et al. 2014; Willrodt et al. 2014; Yang et al. 2013; Zhang et al. 2014) was shown to be limited by the low solubility, volatility, and toxicity of the products (and intermediates) as well as a poor terpene precursor supply via the native methylerythritol phosphate pathway. An increase of terpene precursor concentrations was achieved by the introduction of the mevalonate (MVA) pathway in *E. coli* followed by optimization of promotor strength (Anthony et al. 2009), codon usage (Redding-Johanson et al. 2011), translation initiation (Nowroozi et al. 2014), and gene selection (Ma et al. 2011; Yang et al. 2012) and resulted in the formation of aliphatic (mono-) terpenes from glucose. Recombinant strains carrying cytochrome P450 monooxygenase 153A6 or cymene monooxygenase (CymA), both of bacterial origin, enabled the regioselective biotransformation of limonene to perillyl alcohol (POH) (Cornelissen et al. 2013; Mars et al. 2001; van Beilen et al. 2005). However, due to the inherent complexity of oxygenase systems (Bernhardt and Urlacher 2014) and the physical properties of the (mono-) terpene educts, a direct coupling of the oxygenation reaction to the fermentation is very difficult (Alonso-Gutierrez et al. 2013). Gene-based engineering strategies, successful for the optimization of the heterologous MVA pathway, can be complemented with reaction engineering or novel fermentations concepts meeting the special requirements given by the involved compounds and enzymes. Typically, the toxicity of monoterpenes is counteracted by the use of biphasic setups, additionally facilitating downstream processing by in situ product removal (Frohwitter et al. 2014; Newman et al. 2006). The fermentative production of monoterpenes was shown to profit from the addition of diisononyl phtalate (DINP) (Willrodt et al. 2014) or dodecane (Sarria et al. 2014). However, for the direct microbial production of perillyl alcohol from glucose via limonene, the application of an aqueous:organic two-liquid phase system was counterproductive as the formed limonene was efficiently extracted into the organic carrier phase making it unavailable for oxyfunctionalization

(Alonso-Gutierrez et al. 2013). The objective of this study was to overcome factors preventing the de novo synthesis of perillyl acetate, which can be readily converted to perillyl alcohol by saponification (Štekrová et al. 2012), with engineered *E. coli* (Fig. 1). Engineering strategies addressing parameters such as oxygenase concentration, spatial enzyme proximity, and enzyme kinetics or localization enabled coupling of the limonene oxygenation step to limonene production in a two-liquid phase system, but still identified the intracellular limonene availability as the main limiting factor. Inspired by the orthologous nature of the biosynthesis pathway, we finally developed a novel fermentation concept spatially separating limonene formation from glucose and its oxygenation using a defined mix of two distinct cultures of non-growing cells in a monophasic cultivation system.

Materials and Methods

Chemicals, oligonucleotides, and bacterial strains. Anhydrous D-glucose was obtained from Alfa Aesar (Karlsruhe, Germany), and isopentenyl diphosphate (IPP), dimethylallyl diphosphate (DMAPP) and geranyl diphosphate (GPP) were purchased from Echelon Biosciences (Salt Lake City, UT, USA) at a purity of >95%. Custom synthesized oligonucleotides were purchased from Sigma Aldrich (Steinheim, Germany). Perillyl acetate (>98.8% purity) was kindly provided by Hiroshi Tsuda (Nippon Terpene Chemicals, Inc., Tokyo, Japan). All other chemicals were obtained from AppliChem (Darmstadt, Germany), Sigma Aldrich (Steinheim, Germany), or Carl Roth (Karlsruhe, Germany) at the highest purity available. *E. coli* strains and plasmids used are listed in Tab. I. The details of vector architecture and primer design are provided in the Supporting Information (Fig. S1, Tab. SI, supporting text).

Cultivation of *E. coli* strains. *E. coli* strains were cultivated as described before (M9* medium, baffled Erlenmeyer flasks, liquid:gas phase ratio of 1:4) (Willrodt et al. 2014). Cultures were incubated at 30 °C (200 rpm, 2.5 cm amplitude). Recombinant gene expression was induced by

adding 1.0 mM isopropyl β-D-1-thiogalactopyranoside (IPTG) or 0.025% (v/v) dicyclopropyl ketone (DCPK). If required, ampicillin, gentamicin, and/or chloramphenicol were added at concentrations of 100, 10, and 34 mg L^{-1}, respectively. Thiamine (if appropriate) and δ-aminolevulinic acid (heme synthesis) were added to final concentrations of 0.001% (w/v) and 0.5 mM, respectively.

Analytical procedures. Cell growth was monitored by measuring the optical density at 450 nm (Libra S11, Biochrom Ltd., Cambridge, UK, OD_{450} = 1 equals 0.166 g_{cdw} L^{-1}) (Blank et al. 2008). For two-liquid phase fermentations, cells were washed once with potassium phosphate buffer (KP_i, 0.1 M, pH 7.4) prior to OD_{450} determination, because the presence of DINP increased the OD_{450} value. The concentrations of (*S*)-(-)-limonene, (*S*)-(-)-perillyl alcohol, (*S*)-(-)-perillyl aldehyde, and perillic acid were determined using a GC method described previously (Willrodt et al. 2014). GC-based quantification of (*S*)-(-)-perillyl acetate was done as follows: splitless injection, 80°C (5 min), 80 – 160°C (7.5°C min^{-1}), 160 – 300°C (40°C min^{-1}), 300°C (5 min).

Fermentatively produced limonene and POHAc were identified by comparison with authentic standards and by GC-MS using a CP3800 GC coupled to a 1200 Quadrupole MS (Varian, Inc., Palo Alto, CA, USA) using the same settings as described above.

Resting cell assays (biotransformation). Cells were grown in M9* medium at 30°C as described above. At desired time points after induction, the cells were harvested by centrifugation (4°C, 4,618 g, 20 min) and resuspended to approximately 1 g_{cdw} L^{-1} (OD_{450} = 1 equals 0.166 g_{cdw} L^{-1}) in 0.1 M potassium phosphate buffer pH 7.4 with 1.5% (w/v) glucose. Absence of growth was deduced from OD_{450} measurements. Limonene biotransformation assays were performed as described before (Cornelissen et al. 2011). Due to evaporation, limonene could not be quantified in monophasic resting cell assays. For two-liquid phase biotransformation resting cell assays, the preceding culture was supplemented with 0.5% (w/v) yeast extract to accelerate growth. Resting

cell suspensions of 1 mL were incubated for 5 min (300 rpm, 30°C, Aquatron, Infors, Bottmingen, Switzerland), before addition of limonene in 0.5 mL DINP (initial concentrations are specified in results section). The reaction was terminated after 2 h by centrifugation (4°C, 4,618 g, 10 min). One hundred µL of the organic phase were diluted in 900 µL Et_2O (with 0.2 mM dodecane as internal standard), dried over anhydrous Na_2SO_4, and analyzed for product formation via GC.

CO difference spectra. The specific CYP153A6 content was determined as described previously (Cornelissen et al. 2011). Here, 0.5 mL of the cell suspension (~3.3 g_{cdw} L^{-1} in 0.05 M $KP_{i,}$ pH 7.4) were mixed with 0.4 mL KP_i (0.05 M, pH 7.4) and 0.1 mL $Na_2S_2O_4$ solution (200 mM).

In vitro activity assays. In vitro activity assays were performed as described elsewhere (Willrodt et al. 2014), with the following modifications: The cells were harvested 20 h after induction of recombinant gene expression and the total protein content was either set to 5 $g_{protein}$ L^{-1} (IPP/DMAPP as substrates) or to 0.5 $g_{protein}$ L^{-1} (GPP as substrate). Fifty µL from respective substrate stocks (in methanol) were added to 0.5 mL of the protein solution, resulting in final concentrations of 250 µM IPP and DMAPP or 500 µM GPP.

Fermentative perillyl acetate production with growing cells. Recombinant *E. coli* strains were cultivated in screw-capped baffled flasks. If desired, DINP was added upon induction at an aqueous:organic phase ratio of 4:1 to avoid limonene evaporation. The organic phase was analyzed as described. Aliquots of the aqueous phase were extracted by the addition of an equal volume ice-cold Et_2O (with 0.2 mM dodecane as internal standard), dried over Na_2SO_4, and analyzed by GC.

Fermentative limonene and perillyl acetate production in mixed-strain resting cell assays. *E. coli* BL21 DE3 (pMVAidi, pTAC:LS:AGPPS2), *E. coli* MG1655 (pTAC:POH), and *E. coli* MG1655 (pTAC:CymA) were cultivated as described above. Gene expression was induced at an OD_{450} of 0.6 to 0.8 and cultivation was continued for 12 h after induction. Subsequently, the cells were harvested (4°C, 4,618 g, 20 min), washed with ice-cold potassium phosphate buffer (0.1 M,

pH 7.4), resuspended in the same buffer and combined at different cell densities (specified in text). To assess limonene formation in resting cell fermentations, different strains of *E. coli* (pMVAidi, pTAC:LS:AGPPS2) were used as single strains and DINP was added to avoid limonene evaporation (aqueous:organic phase ratio 4:1). The cell suspensions (25 mL in 250 mL screw-capped baffled flasks) were adapted for 15 min in a rotary incubator (30°C, 200 rpm, 2.5 cm amplitude). Product formation was initiated by adding 0.75 mL glucose (50% (w/v)) and analyzed after extraction of the aqueous phase with Et_2O or after dilution of the organic phase with Et_2O (see above).

Results

Efficient extraction of limonene limits perillyl alcohol formation. The de novo biosynthesis of POHAc (and POH) was shown to be limited by efficient extraction of limonene in a two-liquid phase fermentation system, which could be relieved by omission of the organic carrier phase partially (Alonso-Gutierrez et al. 2013). However, here batch cultivation of different limonene producing *E. coli* strains (DH5α, BL21 (DE3), MG1655) (Willrodt et al. 2014) that were co-transformed with a third plasmid harboring CYP153A6 monooxygenase (pCom8:PFR1500) (van Beilen et al. 2005) did not lead to detectable amounts of POHAc. POHAc was neither detected in a monophasic nor in a biphasic cultivation system applying DINP as organic carrier phase. Limonene, however, accumulated in the organic phase (data not shown). The maximum specific CYP153A6 concentration was 40 nmol g_{cdw}^{-1}. Thus, all genes involved were expressed functionally, but, as described before, limonene was efficiently extracted into the organic phase (Alonso-Gutierrez et al. 2013) which seemed to result in a mass transfer limitation for the oxygenation. The high partition coefficient of $(24.0 \pm 2.7) \times 10^3$ for limonene in DINP/water supports this hypothesis. To determine the concentration of limonene in the organic phase enabling limonene hydroxylation formation, biotransformations with fully induced non-growing *E. coli*

W3110 (pCom8:PFR1500) were performed in a DINP/medium mixture (organic:aqueous phase ratio 1:2) with different limonene concentrations (0.5, 1, 2, 4, 8, 16, 32, 64, 128, 256 mM). Limonene hydroxylation started at limonene concentrations between 64 and 125 mmol L_{org}^{-1} (Fig. 2). Using *E. coli* W3110 (pCom8:PFR1500L) with an improved uptake of hydrophobic molecules into the cell due to the presence of AlkL (Cornelissen et al. 2013; Julsing et al. 2012b), at least 16 to 32 mmol L_{org}^{-1} of limonene were required for hydroxylation (Fig. 2). As those minimally required concentrations are well above the reported 0.74 mmol L_{org}^{-1} limonene produced from 1% (w/v) glucose (Willrodt et al. 2014), POH and consequentially also POHAc formation in the applied experimental two-liquid phase setup, is infeasible and might be hindered by the amount or kinetic properties of the monooxygenase. Therefore, we here focused on the influence of the monooxygenase as a complementary strategy to the approach described by Alonso-Gutierrez et al. who aimed at increasing the terpene precursor supply by genetic pathway engineering (Alonso-Gutierrez et al. 2013). Three potential strategies were defined to achieve POHAc formation from glucose in a two-liquid phase setup: (i) combination of all downstream pathway genes (for LS, AGPPS2, CYP153A6 with redox partners) in one operon to temporally couple their expression and potentially optimize the intracellular CYP153A6 concentration, (ii) generation of a translational fusion of LS and CYP153A6 to establish spatial proximity of limonene formation and oxygenation, and (iii) application of CymA from *P. putida* as an alternative limonene hydroxylase.

First, we assessed each strategy individually with respect to the functional expression of the downstream genes converting the terpene precursors IPP and DMAPP to limonene and POH. In order to investigate recombinant strains for limonene hydroxylation capability the POH formation rate in resting cells by externally adding limonene served as an important measure. Together with the CO difference spectra, revealing the specific CYP153A6 content, these activities allowed for

reliable selection of optimal expression conditions for CYP153A6 with respect to expression time and host. Furthermore, in vitro assays supplying IPP and DMAPP were applied as a measure to investigate the formation of limonene and oxygenated adducts in an extracellular environment and to verify the successful expression of all downstream genes. Subsequently, the strains harboring the entire POHAc formation pathway (MVA pathway, LS; AGPPS2, monooxygenase) were tested for de novo POHAc synthesis.

Simultaneous expression controlled by the P_{tac} promotor improves CYP153A6 availability. In order to tackle the low specific CYP153A6 content of the three-plasmid system (max 40 nmol g_{cdw}^{-1}) as compared to the single plasmid system (163 nmol g_{cdw}^{-1} (Cornelissen et al. 2013)), the genes encoding the CYP153A6 system, LS and AGPPS2 were assembled in one operon. This modification resulted in high specific limonene hydroxylation activities (up to 6.8 U g_{cdw}^{-1}) and improved specific CYP153A6 concentrations (up to 183 nmol g_{cdw}^{-1}) for both *E. coli* MG1655 (pTAC:POH) and *E. coli* MG1655 (pTAC:POH, pMVAidi) (Fig. 3 **A, B**). *E. coli* MG1655 was chosen as the preferred host, as it showed, compared to other *E. coli* strains, the highest maximum specific CYP153A6 content (data not shown) and was shown to be suitable for fermentative limonene production (Willrodt et al. 2014). The limonene hydroxylation activity was coupled to the growth stage of the culture and could be sustained for as long as 20 h after induction. The specific CYP concentration (Fig. 3**A**) and limonene hydroxylation activity (Fig. S2) decreased after glucose depletion. During short term (5-10 min) resting cell assays to assess the limonene oxygenation rate, POH (and minor amounts of perillyl aldehyde) were the only limonene oxidation products. Possibly, the activity of the chloramphenicol acetyltransferase (CAT), encoded on pMVAidi and hypothesized to be responsible for the acetylation of POH (Fig. S3, (Alonso-Gutierrez et al. 2013)), was too low to generate detectable amounts of POHAc in this short time frame. To verify the functionality of all downstream enzymes in concert, extracts from induced

E. coli MG1655 (pTAC:POH) and *E. coli* MG1655 (pTAC:POH, pMVAidi) were analyzed for terpene formation after addition of terpene precursors in an aqueous single phase system. For MG1655 (pTAC:POH, pMVAidi) extracts supplied with IPP/DMAPP, a limonene formation rate of 2.4 ± 0.0 U $g_{protein}^{-1}$ (Fig. 3**C**) and an initial POH formation rate of 0.72 ± 0.02 U $g_{protein}^{-1}$ were found. The latter rate, however, might have been limited by the availability of NADH, which was not externally supplied to the assay. A significantly higher limonene formation rate of 33.2 ± 0.2 U $g_{protein}^{-1}$ was found with GPP as substrate (Fig. 3**C**). Formation of POH was not observed in this experiment, due to the lower protein concentration applied. However, all proteins responsible for the formation of POH from IPP and DMAPP were synthesized simultaneously and functionally from pTAC:POH.

Functional fusion of LS and CYP153A6. To minimize limonene extraction prior to its hydroxylation, we brought LS and CYP153A6 into spatial proximity by generating a translational fusion connecting the two enzymes via a flexible amino acid linker (GGGGGGA). *E. coli* MG1655 (pTAC:POHf) showed similar growth as compared to the strain harboring pTAC:POH. Approximately 3-fold lower maximum specific CYP153A6 concentrations were found for strains containing the hybrid LS-CYP153A6 compared to the non-fused enzymes (Fig. 3**A, B** and Fig. 4**A, B**). The maximum specific limonene hydroxylation activities were 6 U g_{cdw}^{-1} for both strains with the LS-CYP153A6 fusion (Fig. 4**A, B**). Extracts from *E. coli* MG1655 (pTAC:POHf, pMVAidi) showed similar reaction rates for the two-step bioconversion (IPP/DMAPP to limonene) as compared to extracts from *E. coli* MG1655 (pTAC:POH, pMVAidi). The specific reaction rate for the one step bioconversion (GPP to limonene) was impaired and found to be approximately 2.8-fold lower for the LS-CYP153A6 hybrid (Fig. 4**C**). The specific POH formation activity with IPP/DMAPP as substrates was 0.36 U $g_{protein}^{-1}$ using extracts of *E. coli* MG1655 (pTAC:POHf, pMVAidi). Although, no improvement of product formation was observed with this specific linker

connecting LS and CYP153A6 in the in vitro assays, the functional coupling of these enzymes was successful and had to be evaluated in vivo.

CymA is a specific and highly active limonene hydroxylase. To investigate an alternative limonene hydroxylase with putatively improved properties, the genes for the monooxygenase CymAa and the respective reductase CymAb (Eaton 1997) were amplified from the genomic DNA of *P. putida* GS1 and cloned behind the P_{tac} promotor of pTAC giving pTAC:CymA. High and stable limonene hydroxylation activities of approximately 10 U g_{cdw}^{-1} (for $\geq$ 1 h) were observed with resting *E. coli* MG1655 (pTAC:CymA) cells harvested 4 h after induction (data not shown). After verification of the CymA activity in this bicistronic expression system, *cymAa* and *cymAb* were sub-cloned into pTAC:LS:AGPPS2 yielding pTAC:POH:CymA. To ensure comparability with the CYP153A6 containing strains, pTAC:POH:CymA was assembled with the similar gene order as pTAC:POH (LS, monooxygenase, AGPPS2, redox partner; see Supplemental Information for details). Resting *E. coli* MG1655 (pTAC:POH:CymA, pMVAidi) showed very high limonene hydroxylation rates of 17.9 ± 0.9 U g_{cdw}^{-1}, demonstrating the functional expression of the CymA gene from pTAC:POH:CymA. A product mixture of POH and perillyl aldehyde (roughly 50:50) was obtained.

Perillyl acetate is synthesized from glucose. *E. coli* MG1655 harboring pMVAidi in combination with either pTAC:POH, pTAC:POHf, or pTAC:POH:CymA were tested for in vivo POHAc formation from glucose. Indeed, the accumulation of POHAc was observed as a result of POH acetylation catalyzed by the chloramphenicol acetyl transferase encoded on pMVAidi (Fig. S3). Low amounts of POHAc (maximally ~37 µmol L_{aq}^{-1} or ~6.6 mg L_{aq}^{-1}) were found for *E. coli* MG1655 (pTAC:POH, pMVAidi) 48 h after induction (Fig. 5). Notably, a similar POHAc formation also was observed in the two-liquid phase setup, demonstrating that the intracellular CYP153A6 amount, in contrast to the 3 plasmid system, was sufficient to allow limonene

hydroxylation prior to extraction into the organic carrier phase. The coexpression of the *cymA* genes led to significantly less formation of POHAc. This is caused by the significantly reduced limonene synthesis (Fig. 5), possibly the result of impaired AGPPS2 synthesis (SDS-PAGE analysis, Fig. S4). Further POH oxidation products (perillyl aldehyde and perillic acid) were also not observed. The highest specific POHAc yields were found for *E. coli* MG1655 (pMVAidi, pTAC:POH) in a two-liquid phase system with 6.20 ± 0.06 mg g_{cdw}^{-1} and 0.68 ± 0.03 mg $g_{glucose}^{-1}$. Despite successful hydroxylation of produced limonene, the titers obtained were low and make a detailed assessment of the product formation kinetics difficult. Furthermore, the majority of produced limonene accumulated in the organic phase or evaporated, pointing to intrinsic physical properties of limonene still limiting the hydroxylation in the experimental setup applied. As the extrusion of limonene could not be prevented, we sought to develop a fermentation setup that takes advantage of this obviously inevitable phenomenon.

Defined multi-strain mixed cultures of non-growing cells produce POHAc at high rates. In general, growing cells are applied for terpene production from glucose (Ajikumar et al. 2010; Martin et al. 2003). Resting (non-growing, but metabolically active) cells are frequently applied for biotransformations and often show higher product formation rates as their growing counterparts (Julsing et al. 2012a). Here, the potential of resting cells for the fermentative production of terpenes was investigated. In a preliminary experiment aiming at establishing the preconditions we observed that resting cells of different *E. coli* strains harboring pTAC:LS:AGPPS2 and pMVAidi showed higher limonene formation rates (~0.3 U g_{cdw}^{-1}, Fig. 6**A**) as compared to growing cells (~0.1 U g_{cdw}^{-1}, (Willrodt et al. 2014)). This preliminary experiment also identified *E. coli* BL21 DE3 (pTAC:LS:AGGPS) as the most suitable host for resting cell limonene fermentation. *E. coli* BL21 DE3 however, showed the lowest expression of functional CYP153A6 (data not shown). Therefore, we decided to directly examine the best host

for functional CYP153A6 synthesis *E. coli* MG1655 transformed with pTAC:POH and pMVAidi for fermentative POHAc formation with resting cells. Indeed, POHAc was observed, however, at very low final concentrations and specific formation rates (initially ~10 mU g_{cdw}^{-1}) (Tab. II, Fig. 6**B**). Surprisingly, limonene accumulation was not detected during this experiment, which raised question whether it would be possible to selectively increase limonene biosynthesis by increasing the amount of limonene producing biomass. For this, we developed a mixed-strain resting cell approach for the fermentative synthesis of limonene oxidation products by combining a strain producing limonene with a separate strain for limonene oxygenation. To this end, *E. coli* BL21 DE3 (pTAC:LS:AGPPS2, pMVAidi) and *E. coli* MG1655 (pTAC:POH), respectively, were cultivated in separate shaking flasks from which mixed-strain cell suspensions with a ratio 10 g_{cdw} L^{-1} (limonene producer) and 1 g_{cdw} L^{-1} (limonene hydroxylation) were composed. POHAc accumulated as the sole limonene oxidation product. The specific product formation rate (Fig. 7**A**) remained constant for ~3 h and decreased afterwards due to glucose depletion. The overall specific production rates were slightly higher when cell mixtures of 5, 2.5, or 1 g_{cdw} L^{-1} limonene producing and 1 g_{cdw} L^{-1} limonene hydroxylating cells were applied, which is in contrast to the reduced volumetric activity for limonene formation (Fig. 7A). Normalizing the POHAc formation rate to the applied biomass harboring the CYP153A6 enzyme (1 g_{cdw} L^{-1}) resulted in the highest specific limonene hydroxylation (which in this case is equal to the volumetric productivity) rate of 0.60U g_{cdw}^{-1} in the 10:1 system (Fig. 7**B**). POHAc formation in the fermentations applying the 2.5:1 and the 1:1 ratio ceased 120 minutes after beginning of the fermentation (data not shown) and therefore these low cell densities were rendered inappropriate for efficient POHAc synthesis due to limiting limonene availability. In all assay setups, limonene accumulated in the aqueous phase (and the headspace), though only trace amounts for the 2.5:1 and the 1:1 experiment. The observed limonene concentrations (altering over time, maximum 46 µM after 2 h, 10 g_{cdw} L^{-1}

limonene producing cells) were well below the uptake constant K_S (defined as the substrate concentration that results in the half-maximum product formation rate) of 109 ± 3 µM (determined for *E. coli* MG1655 harboring pTAlk:POH, Fig. S5). Thus, for the higher cell densities applied (10 or 5 g_{cdw} L^{-1} of limonene producing cells) POHAc formation might be limited by limonene uptake by the cells containing CYP153A6. Compared to the approach using growing cells, the mixed-strain fermentations achieved a 3.3-fold higher final POHAc concentrations (~125 µmol L_{aq}^{-1} or ~22 mg L_{aq}^{-1}) in a shorter time period of less than 3 h, but with significantly higher biomass concentrations (Tab. II). The high biomass concentration and the excess of limonene producing cells were crucial to ensure sufficiently high limonene concentrations for the subsequent oxyfunctionalization over the entire fermentation time frame.

In order to evaluate CymA in the mixed-strain resting cell setup, the combination of limonene producing cells and *E. coli* MG1655 (pTAC:CymA) (1 g_{cdw} L^{-1}) resting cells was investigated. The overall specific perillyl acetate formation rate and volumetric activity were increased when 10 instead of 5 g_{cdw} L^{-1} limonene producing cells were applied (Fig. 7**C, D**). Furthermore, limonene only accumulated when a cell concentration of 10 g_{cdw} L^{-1} of the limonene producer were used. Obviously, CymA performed better in the mixed- strain approach as compared to CYP153A6.

Discussion

Production of oxygenated limonene derivatives in a two-liquid phase system. The fermentative production of monoterpenes has multiple challenges determined by their physico-chemical properties such as volatility (van der Werf et al. 1997), relatively low water solubility (11 - 53 µmol L^{-1} (Schmid et al. 1992)) and high toxicity towards typical microbial production hosts (logP values of around 4.5). Limonene concentrations exceeding 0.025% (v/v) were shown to completely inhibit the growth of *E. coli* (Dunlop et al. 2011). These drawbacks can be relieved by

the use of a two-liquid phase fermentation setup. However, for the production of oxygenated derivatives the extraction of limonene into an organic carrier phase is kinetically favored over its oxygenation. Thus, the intracellular coupling of an oxygenation reaction to the synthesis of monoterpenes requires a tradeoff between monoterpene toxicity and sufficiently high intracellular monoterpene concentrations. At this point, metabolic engineering strategies aiming at the optimization of intracellular protein levels is a possible, but very challenging approach. Other potential approaches are channeling of intermediates or improvement of enzyme kinetics.

CYP153A6 shows a roughly 20-fold higher catalytic efficiency (k_{cat}/K_M = 0.111 μM^{-1} s^{-1} (Funhoff et al. 2006)), than LS (Williams et al. 1998). Thus, a strategy aiming at the optimization of kinetic parameters seems to be inappropriate and the focus should be on increasing the intracellular CYP153A6 concentrations. Indeed, increasing the intracellular CYP153A6 concentration (with pTAC:POH) did allow for the direct oxygenation of fermentatively synthesized limonene during batch fermentation of *E. coli* MG1655 (pTAC:POH, pMVAidi) in a two-liquid phase system, albeit at rather low titers. In this context, a further increase in specific CYP153A6 content in recombinant *E. coli* might be difficult as the obtained CYP153A6 concentration (187 nmol g_{cdw}^{-1} for *E. coli* MG1655 harboring pTAC:POH) is close to reported 200 nmol g_{cdw}^{-1} (Olaofe et al. 2013) and 249 nmol $gcdw^{-1}$ (Cornelissen et al. 2013).

Substantial amounts of limonene accumulated in the organic phase, showing that limonene extraction remained the most critical issue. Interestingly, the same POHAc levels (calculated per aqueous phase volume) were obtained for both mono- and biphasic batch cultivations of *E. coli* MG1655 (pTAC:POH, pMVAidi) suggesting that the extrusion of limonene into the extracellular environment prior to oxygenation is not facilitated by the addition of an organic phase. The extraction of limonene into the organic phase has been reported as the main obstacle for POH production (Alonso-Gutierrez et al. 2013). Here, we identified the extraction of limonene into the

organic and/or evaporation into the gaseous phase, and thus intracellular limonene availability, as the key issue for effective oxygenation.

Although, we intended to increase production of POHAc by the generation of a functional LS-CYP hybrid protein, the total POHAc production was much lower in the final recombinant strain (pTAC:POHf, pMVAidi) as compared to the non-fusion control strain (pTAC:POH, pMVAidi) (Fig. 6). A reduced synthesis of the fusion protein led to a reduced limonene synthesis rate and consequentially to a lower final POHAc concentration. Nonetheless, the molar limonene/POHAc ratio decreased from 3.2 for *E. coli* MG1655 (pTAC:POH, pMVAidi) to 1.6 for *E. coli* MG1655 (pTAC:POHf, pMVAidi), both in a two-liquid phase system, pointing at an improved coupling of limonene synthesis and its oxyfunctionalization. The applied oligo-Gly (GGGGGGA) linker was chosen based on its flexibility (Argos 1990) and the length was kept short to minimize diffusion distance. In this context, a (rational) optimization of the linker sequence and length has potential as an approach to increase expression/activity of both fusion partners (Chen et al. 2013).

Although considerable progress regarding the formation of oxygenated limonene derivatives in a two-liquid phase setup was achieved, the POHAc titers were rather low and a systematic quantitation of the production capacity and rates of the system was difficult.

The construction of orthologous recombinant pathways is often performed in a straightforward manner using the advantage that the pathway typically is not influenced by the endogenous regulatory network. However, this and other studies (e.g., (Dahl et al. 2013; Nowroozi et al. 2014)) showed that orthologous pathway development requires more than the assembly of the necessary genes and functional modules. Fine-tuned enzyme synthesis, enzymatic properties, physical phenomena, such as mass transfer, and most importantly, the intrinsic properties of reaction intermediates and products have to be considered.

Mixed-strain resting cells: A promising approach for difficult fermentations For redox biotransformations, the application of whole cells is beneficial in terms of enzyme stabilization in the cellular environment, redox-equivalent supply, and self-regeneration (Schrewe et al. 2013). Resting cells, however, typically show limited stability and self-regeneration, but do not produce biomass as by-product that competes with the biocatalytic pathway for carbon and energy. Indeed, increased redox-cofactor regeneration and product formation rates have been observed in non-growing cells (Blank et al. 2008; Julsing et al. 2012a). Approaches that use metabolically active non-growing cells harboring a heterologous pathway for the production of value-added compounds from cheap carbon sources (fermentation), however, are rare (Wittgens et al. 2011). We showed that the formation of limonene, via the heterologous MVA pathway can be decoupled from biomass formation, and developed a novel fermentation concept using mixed strains for the coupling of an oxygenation reaction to fermentatively produce the limonene derivative POHAc.

With the mixed culture resting cell concept a 3.3-fold higher POHAc concentration was achieved as compared to the single strain two-liquid phase fermentation (Tab. II). The comparison of the productivity, however, is more difficult and suffers from the unknown POHAc formation kinetics during the batch cultivation, which could not be assessed quantitatively due to the low POHAc concentrations obtained. The calculated productivity should therefore be interpreted with care. If 4 h of pre-induction phase and 12 h of late stationary phase were subtracted as being non-productive for the batch fermentation an up to ~34-fold (to ~7.3 mg L^{-1} h^{-1}) improved productivity was observed for the mixed-culture resting cell setup. This seemed to be a consequence of the higher cell density applied and the relieved limonene limitation. Upscaling the batch fermentation from shake flasks to a bioreactor setup allows significantly increased biomass concentrations, which might enable a systematic analysis of POAHc formation with growing cells and thus an accurate determination of the productivity. This however was beyond the scope of the present

study. The lower specific POHAc yield in the mixed-strain setup might be improved by additional glucose supplementation and continued production. However, for this, the stability of the resting cell activity has to be determined and possibly improved by the optimization of for example medium composition or temperature. Additionally, an oxygen limitation for both cellular maintenance (energy supply via respiration) and the oxygenation reaction cannot be excluded, especially when high cell concentrations are applied. Thus, it should be noted that the presented system is running at sub-optimal conditions offering multiple opportunities for optimization.

The main advantages of the mixed-culture concept are the possibility to titrate production rates of different steps by adjusting the ratio of the respective cell numbers of each strain and selecting optimum expression conditions (host, expression time etc.) for the enzymes involved. This especially becomes evident when comparing to the single-strain resting cell performances. Taking advantage of the excess of limonene producing cells and the higher limonene biosynthesis rate of *E. coli* BL21 DE3 as compared to MG1655 (Fig. 6A), the final POHAc concentration and the specific POHAc yield could be improved 12 and 9-fold, respectively as compared to the single-strain resting cell fermentation (Tab. II). By artificially increasing the volumetric limonene synthesis rate (increasing the amount of limonene producing cell) we could show that limonene availability is a limiting factor for hydroxylation. In this experimental setup the limonene availability is influenced by (i) the rate of limonene biosynthesis, (ii) the rate of limonene evaporation into the headspace, and (iii) the rate of limonene hydroxylation, which in turn are determined by mass transfer rates and enzyme kinetics. By having the opportunity to manually control the biocatalyst stoichiometry and biomass concentrations one might be able to identify improved production conditions, which is part of ongoing research. Analogous advantages have been described for complex in vitro enzyme cascades (Bujara et al. 2011; Myung et al. 2014; Zhang et al. 2010), but not yet for fermentative whole-cell biocatalysis. The versatility of this

approach was proven by the use of two different enzyme systems (CYP153A6 and CymA) catalyzing the regioselective limonene oxyfunctionalization. CymA performed significantly better than CYP153A6 in terms of the total POHAc formation. CymA is hypothesized to be located in the cytoplasmic membrane (Eaton 1997). Increased local limonene concentrations in the cytoplasmic membrane may contribute to a better performance with CymA, which is also reflected by the whole-cell biotransformation kinetics. For both biocatalysts (harboring either CYP153A6 or CymA) similar substrate uptake constants (K_S of approximately 100 µmol L^{-1}) were observed, but a significantly higher V_{max} was obtained with CymA (Fig. S5). However, also the K_S (and K_M) value of the catalysts for oxygen must not be disregarded.

Based on these findings, it is likely that the limonene mass transfer rate over the outer membrane limits the hydroxylation, as the outer membrane is believed to be an efficient barrier for hydrophobic molecules (Chen 2007). This mass transfer issue could be counteracted by the introduction of the hydrophobic-pore protein AlkL into the cell performing the oxygenation. AlkL was shown to increase the uptake of limonene, alkanes, and fatty acid methyl esters in whole cell biotransformations (Cornelissen et al. 2013; Julsing et al. 2012b). Finally, the electron transfer in the three component CYP153A6 system might be less efficient in terms of coupling as compared to the two component CymA enzyme system.

Another optimization strategy could aim at exchanging the chloramphenicol acetyltransferase gene for another selection marker might be considered, since omission of this gene would lead to the formation of POH as the sole oxygenation product. However, overexpression of CAT might generate a metabolic pull mechanism for more efficient POHAc synthesis.

The spatial dissection of the fermentative formation of a terpene from its hydroxylation constitutes a modularization approach which allows the construction/assembly of different synthetic reaction cascades, e.g., using different hydroxylases, without the need for elaborate genetic pathway

engineering and balancing. The presented approach has multiple benefits, but also downsides and limitations. The long term stability (>3 h) and the artificial introduction of mass transfer barriers for the limonene intermediate (by separating limonene production and hydroxylation in different cells) are considered most critical.

Conclusion

The availability of highly volatile limonene for the monooxygenase was found to limit fermentative POH/POHAc production. Three strategies were evaluated for POHAc synthesis in a two-liquid phase system. Increasing the specific CYP153A6 concentration was found suitable to lower limonene extraction prior to its oxygenation. Furthermore, a novel mixed-strain resting cell-fermentation concept was developed with the cell number/strain-ratio as a powerful and tunable parameter. This concept enabled effective POHAc production with two different limonene hydroxylase systems (CYP153A6 and CymA). The approach is complementary to and can be combined with metabolic engineering. Mixed-culture resting cell fermentations may serve as general tools to perform cascade reactions involving intermediates and products in multistep reactions with challenging properties like high volatility and toxicity, and low solubility.

Acknowledgements

We gratefully thank J. B. van Beilen and B. Witholt for providing the plasmid pCom8:PFR1500. Sjef Cornelissen is acknowledged for providing the plasmid pCom8PFR1500L. This project was partially financed by the Deutsche Bundestiftung Umwelt (DBU: AZ13252).

References

Ajikumar PK, Xiao WH, Tyo KE, Wang Y, Simeon F, Leonard E, Mucha O, Phon TH, Pfeifer B, Stephanopoulos G. 2010. Isoprenoid pathway optimization for Taxol precursor overproduction in *Escherichia coli*. Science 330(6000):70-74.

Alonso-Gutierrez J, Chan R, Batth TS, Adams PD, Keasling JD, Petzold CJ, Lee TS. 2013. Metabolic engineering of *Escherichia coli* for limonene and perillyl alcohol production. Metab Eng 19(9):33-41.

Anthony JR, Anthony LC, Nowroozi F, Kwon G, Newman JD, Keasling JD. 2009. Optimization of the mevalonate-based isoprenoid biosynthetic pathway in *Escherichia coli* for production of the anti-malarial drug precursor amorpha-4,11-diene. Metab Eng 11(1):13-19.

Argos P. 1990. An investigation of oligopeptides linking domains in protein tertiary structures and possible candidates for general gene fusion. J Mol Biol 211(4):943-958.

Bernhardt R, Urlacher VB. 2014. Cytochromes P450 as promising catalysts for biotechnological application: chances and limitations. Appl Microbiol Biotechnol 98(14):6185-6203.

Blank LM, Ebert BE, Bühler B, Schmid A. 2008. Metabolic capacity estimation of *Escherichia coli* as a platform for redox biocatalysis: constraint-based modeling and experimental verification. Biotechnol Bioeng 100(6):1050-1065.

Bujara M, Schumperli M, Pellaux R, Heinemann M, Panke S. 2011. Optimization of a blueprint for in vitro glycolysis by metabolic real-time analysis. Nat Chem Biol 7(5):271-277.

Chen RR. 2007. Permeability issues in whole-cell bioprocesses and cellular membrane engineering. Appl Microbiol Biotechnol 74(4):730-738.

Chen X, Zaro JL, Shen WC. 2013. Fusion protein linkers: property, design and functionality. Adv Drug Deliv Rev 65(10):1357-1369.

Cornelissen S, Julsing MK, Volmer J, Riechert O, Schmid A, Bühler B. 2013. Whole-cell-based CYP153A6-catalyzed (*S*)-limonene hydroxylation efficiency depends on host background and profits from monoterpene uptake via AlkL. Biotechnol Bioeng 110(5):1282-1292.

Cornelissen S, Liu S, Deshmukh AT, Schmid A, Bühler B. 2011. Cell physiology rather than enzyme kinetics can determine the efficiency of cytochrome P450-catalyzed C-H-oxyfunctionalization. J Ind Microbiol Biotechnol 38(9):1359-70.

Dahl RH, Zhang F, Alonso-Gutierrez J, Baidoo E, Batth TS, Redding-Johanson AM, Petzold CJ, Mukhopadhyay A, Lee TS, Adams PD and others. 2013. Engineering dynamic pathway regulation using stress-response promoters. Nat Biotechnol 31(11):1039-1046.

Dunlop MJ, Dossani ZY, Szmidt HL, Chu HC, Lee TS, Keasling JD, Hadi MZ, Mukhopadhyay A. 2011. Engineering microbial biofuel tolerance and export using efflux pumps. Mol Syst Biol:10.1038/msb.2011.21.

Eaton RW. 1997. p-Cymene catabolic pathway in *Pseudomonas putida* F1: cloning and characterization of DNA encoding conversion of p-cymene to p-cumate. J Bacteriol 179(10):3171-3180.

Frohwitter J, Heider SA, Peters-Wendisch P, Beekwilder J, Wendisch VF. 2014. Production of the sesquiterpene (+)-valencene by metabolically engineered Corynebacterium glutamicum. J Biotechnol 191(10):205-213.

Funhoff EG, Bauer U, Garcia-Rubio I, Witholt B, van Beilen JB. 2006. CYP153A6, a soluble P450 oxygenase catalyzing terminal-alkane hydroxylation. J Bacteriol 188(14):5220-5227.

Hyatt DC, Youn B, Zhao Y, Santhamma B, Coates RM, Croteau RB, Kang C. 2007. Structure of limonene synthase, a simple model for terpenoid cyclase catalysis. P Natl Acad Sci USA 104(13):5360-5365.
Julsing MK, Kuhn D, Schmid A, Bühler B. 2012a. Resting cells of recombinant *E. coli* show high epoxidation yields on energy source and high sensitivity to product inhibition. Biotechnol Bioeng 109(5):1109-1119.
Julsing MK, Schrewe M, Cornelissen S, Hermann I, Schmid A, Bühler B. 2012b. Outer membrane protein AlkL boosts biocatalytic oxyfunctionalization of hydrophobic substrates in *Escherichia coli*. Appl Environ Microbiol 78(16):5724-5733.
Liese A, Seelbach K, Wandrey C. 2006. Industrial Biotransformations. Weinheim: Wiley-VCH.
Ma SM, Garcia DE, Redding-Johanson AM, Friedland GD, Chan R, Batth TS, Haliburton JR, Chivian D, Keasling JD, Petzold CJ and others. 2011. Optimization of a heterologous mevalonate pathway through the use of variant HMG-CoA reductases. Metab Eng 13(9):588-597.
Mars AE, Gorissen JP, van den Beld I, Eggink G. 2001. Bioconversion of limonene to increased concentrations of perillic acid by *Pseudomonas putida* GS1 in a fed-batch reactor. Appl Microbiol Biotechnol 56(1-2):101-7.
Martin VJ, Pitera DJ, Withers ST, Newman JD, Keasling JD. 2003. Engineering a mevalonate pathway in *Escherichia coli* for production of terpenoids. Nat Biotechnol 21(7):796-802.
Myung S, Rollin J, You C, Sun F, Chandrayan S, Adams MW, Zhang YH. 2014. In vitro metabolic engineering of hydrogen production at theoretical yield from sucrose. Metab Eng 24(7):70-77.
Newman JD, Marshall J, Chang M, Nowroozi F, Paradise E, Pitera D, Newman KL, Keasling JD. 2006. High-level production of amorpha-4,11-diene in a two-phase partitioning bioreactor of metabolically engineered *Escherichia coli*. Biotechnol Bioeng 95(4):684-691.
Nowroozi FF, Baidoo EE, Ermakov S, Redding-Johanson AM, Batth TS, Petzold CJ, Keasling JD. 2014. Metabolic pathway optimization using ribosome binding site variants and combinatorial gene assembly. Appl Microbiol Biotechnol 98(4):1567-1581.
Olaofe OA, Fenner CJ, Gudiminchi RK, Smit MS, Harrison ST. 2013. The influence of microbial physiology on biocatalyst activity and efficiency in the terminal hydroxylation of n-octane using Escherichia coli expressing the alkane hydroxylase, CYP153A6. Microb Cell Fact:10.1186/1475-2859-12-8.
Pham SQ, Pompidor G, Liu J, Li XD, Li Z. 2012. Evolving P450pyr hydroxylase for highly enantioselective hydroxylation at non-activated carbon atom. Chem Comm 48(38):4618-4620.
Pichersky E, Noel JP, Dudareva N. 2006. Biosynthesis of plant volatiles: nature's diversity and ingenuity. Science 311(5762):808-11.
Redding-Johanson AM, Batth TS, Chan R, Krupa R, Szmidt HL, Adams PD, Keasling JD, Lee TS, Mukhopadhyay A, Petzold CJ. 2011. Targeted proteomics for metabolic pathway optimization: application to terpene production. Metab Eng 13(3):194-203.
Sarria S, Wong B, Martin HG, Keasling JD, Peralta-Yahya P. 2014. Microbial Synthesis of Pinene. ACS Syn Biol 3(7):466-475.
Schewe H, Mirata MA, Holtmann D, Schrader J. 2011. Biooxidation of monoterpenes with bacterial monooxygenases. Process Biochem 46(10):1885-1899.
Schmid C, Steinbrecher R, Ziegler H. 1992. Partition coefficients of plant cuticles for monoterpenes. Trees - Struct Funct 6(1):32-36.

Schrewe M, Julsing MK, Bühler B, Schmid A. 2013. Whole-cell biocatalysis for selective and productive C-O functional group introduction and modification. Chem Soc Rev 42(15):6346-6377.

Staunton J, Weissman KJ. 2001. Polyketide biosynthesis: a millennium review. Nat Prod Rep 18(4):380-416.

Štekrová M, Paterová-Dudková I, Vyskočilová-Leitmannová E, Červený L. 2012. Preparation and utilization of perillyl acetate. Res Chem Intermediat 38(8):2075-2084.

van Beilen JB, Holtackers R, Luscher D, Bauer U, Witholt B, Duetz WA. 2005. Biocatalytic production of perillyl alcohol from limonene by using a novel *Mycobacterium* sp. cytochrome P450 alkane hydroxylase expressed in *Pseudomonas putida*. Appl Environ Microbiol 71(4):1737-1744.

van der Werf MJ, de Bont JAM, Leak DJ. 1997. Opportunities in microbial biotransformation of monoterpenes. In: Berger RG, editor. Biotechnology of aroma compounds. Berlin, New York: Springer-Verlag. p 147-177.

Williams DC, McGarvey DJ, Katahira EJ, Croteau R. 1998. Truncation of limonene synthase preprotein provides a fully active 'pseudomature' form of this monoterpene cyclase and reveals the function of the amino-terminal arginine pair. Biochemistry 37(35):12213-12220.

Willrodt C, David C, Cornelissen S, Bühler B, Julsing MK, Schmid A. 2014. Engineering the productivity of recombinant *Escherichia coli* for limonene formation from glycerol in minimal media. Biotechnol J 9(8):1000-1012.

Wittgens A, Tiso T, Arndt TT, Wenk P, Hemmerich J, Müller C, Wichmann R, Kupper B, Zwick M, Wilhelm S and others. 2011. Growth independent rhamnolipid production from glucose using the non-pathogenic *Pseudomonas putida* KT2440. Microb Cell Fact:10.1186/1475-2859-10-80.

Yang J, Nie Q, Ren M, Feng H, Jiang X, Zheng Y, Liu M, Zhang H, Xian M. 2013. Metabolic engineering of *Escherichia coli* for the biosynthesis of alpha-pinene. Biotechnol Biofuels 6(1):60-69.

Yang J, Xian M, Su S, Zhao G, Nie Q, Jiang X, Zheng Y, Liu W. 2012. Enhancing production of bio-isoprene using hybrid MVA pathway and isoprene synthase in *E. coli*. PloS one:10.1371/journal.pone.0033509.

Zhang H, Boghigian BA, Armando J, Pfeifer BA. 2011. Methods and options for the heterologous production of complex natural products. Nat Prod Rep 28(1):125-51.

Zhang H, Liu Q, Cao Y, Feng X, Zheng Y, Zou H, Liu H, Yang J, Xian M. 2014. Microbial production of sabinene - a new terpene-based precursor of advanced biofuel. Microb Cell Fact:10.1186/1475-2859-13-20.

Zhang YH, Sun J, Zhong JJ. 2010. Biofuel production by in vitro synthetic enzymatic pathway biotransformation. Curr Opin Biotechnol 21(5):663-669.

Figure Legends

Figure 1: Biocatalytic de novo synthesis of (*S*)-(-)-perillyl acetate. Glucose is metabolized via the heterologous mevalonate pathway and the IPP/DMAPP isomerase to the terpene precursors isopentenyl diphosphate (IPP) and dimethylallyl diphosphate (DMAPP), which are then condensed by a geranyl diphosphate (GPP) synthase to form GPP. GPP in turn is cyclized via a cationic intermediate to (*S*)-(-)-limonene. The regioselective oxygenation of limonene to perillyl alcohol is catalyzed by the cytochrome P450 monooxygenase 153A6 (CYP153A6). The free alcohol is converted to the respective acetic acid methyl ester perillyl acetate by the chloramphenicol acetyl transferase (CAT), which is present on the plasmid pMVAidi.

Figure 2: Two-liquid phase biotransformation of limonene into perillyl alcohol with resting *E. coli* W3110 (pCom8:PFR1500) (■) and *E. coli* W3110 (pCom8:PFR1500L) (●). The reactions were started by adding 0.5 mL DINP with varying limonene concentrations (0.5, 1, 2, 4, 8, 16, 32, 64, 128, 256 mM) to 1 mL of cell suspensions (~1 g_{cdw} L^{-1}) in glucose containing potassium phosphate buffer. After 2 h, the perillyl alcohol concentration was determined via GC (detection limit: ~5 µM). The error bars relate to results obtained from two independent cultures.

Figure 3: CYP synthesis and activity using the P_{tac} controlled expression of the downstream pathway genes on pTAC:POH. Limonene hydroxylation rates (grey bars in panels **A** and **B**), biomass concentrations (●), and specific CYP contents (■) in dependency of the cultivation time of *E. coli* MG1655 (pTAC:POH) (**A**) or *E. coli* MG1655 (pMVAidi, pTAC:POH) (**B**). The cells were cultivated in M9* minimal medium with an initial glucose concentration of 1% (w/v). In biotransformations with resting cells containing the plasmid pMVAidi with the substrate limonene supplied in excess, POHAc accumulation was not observed. Panel **C**: Specific terpenoid formation rates of crude cell extracts generated 20 h after induction of gene expression in *E. coli* MG1655 (pTAC:POH) (- MVA: without mevalonate pathway) or *E. coli* MG1655 (pMVAidi,

pTAC:POH) (+ MVA: with mevalonate pathway) for the conversion of IPP/DMAPP (IPP) or GPP (GPP) to limonene. The error bars were calculated from results obtained with two independently grown cultures. One unit (U) is defined as one µmol of product formed per minute. The units are either normalized to the total biomass concentration (U g_{cdw}^{-1}) or the total protein concentration (U $g_{protein}^{-1}$). Panel **D**: Schematic drawing of the biocatalytic reactions and CYP153A6. The CYP153A6 structure was obtained via a homology model on the basis of CYP153A7 from *Sphingopyxis macrogoltabida*, PDB ID 3RWL (Pham et al. 2012).

Figure 4: CYP synthesis and activity as part of the LS-CYP hybrid using the P_{tac} controlled expression of the downstream pathway genes on pTAC:POHf. Limonene hydroxylation rates (grey bars in panels **A** and **B**), biomass concentrations (●), and specific CYP contents (■) in dependency of the cultivation time of *E. coli* MG1655 (pTAC:POHf) (**A**) or *E. coli* MG1655 (pMVAidi, pTAC:POHf) (**B**). The cells were cultivated in M9* minimal medium with an initial glucose concentration of 1% (w/v). In biotransformations with resting cells containing the plasmid pMVAidi with the substrate limonene supplied in excess, POHAc accumulation was not observed. Panel **C**: Specific terpenoid formation rates of crude cell extracts generated 20 h after induction of gene expression in *E. coli* MG1655 (pTAC:POHf) (- MVA: without mevalonate pathway) or *E. coli* MG1655 (pMVAidi, pTAC:POHf) (+MVA: with mevalonate pathway) for the conversion of IPP/DMAPP (IPP) or GPP (GPP) to limonene. All error bars were calculated from results obtained with two independently grown cultures. One unit (U) is defined as one µmol of product formed per minute. The units are either normalized to the total biomass concentration (U g_{cdw}^{-1}) or the total protein concentration (U $g_{protein}^{-1}$). Panel **D**: Schematic drawing of the biocatalytic reactions and the functional LS-CYP153A6 fusion. The CYP153A6 structure was obtained as described in the legend of Fig. 4. The structure of limonene synthase (upper protein) was obtained from PDB ID 2ONG (Hyatt et al. 2007).

Figure 5: Monoterpenoid production from glucose with different recombinant *E. coli* MG1655 strains in monophasic (M9* medium) and biphasic (2LP: M9*:DINP phase ratio 4:1) shake flask cultivations. Final

limonene (Lim), perillyl acetate (POHAC), and total monoterpenoid (sum) concentrations are shown. **Lim:** *E. coli* MG1655 (pMVAidi, pTAC:LS:AGPPS2), **CYP:** *E. coli* MG1655 (pMVAidi, pTAC:POH), **LS-CYP** *E. coli* MG1655 (pMVAidi, pTAC:POHf), **CymA:** *E. coli* MG1655 (pMVAidi, pTAC:POH:CymA). For comparability, all concentrations given are translated to the aqueous phase volume and were measured after glucose depletion (approximately after 48 h). Mean values and error bars given refer to three independent cultures.

Figure 6: Resting cell fermentations for limonene and perillyl acetate production. (**A**) Average specific limonene formation rates with resting cells of different *E. coli* strains harboring the limonene biosynthesis pathway (pTAC:LS:AGPPS, pMVAidi). Cells were incubated in a biphasic aqueous:organic (buffer/DINP, 4:1) system with 1.5% (w/v) glucose as sole carbon and energy source. The average rates relate to the increase of limonene during the first 4 h of the resting cell fermentation. (**B**) Time course of POHAc concentration in single strain resting cell fermentations using *E. coli* MG1655 (pTAC:POH, pMVAidi). The cells were grown in M9* medium and gene expression was induced for 12 h. Subsequently, the cells were harvested and resuspended to 8 $g_{cdw}\,L^{-1}$ in potassium phosphate buffer. 1.5% (w/v) glucose was added to initiate monoterpenoid formation. Mean values and error bars given refer to resting cells retrieved from two independent cultures. One unit (U) is defined as one µmol of product formed per minute.

Figure 7: De novo perillyl acetate formation in the mixed-strain resting cell setup. Specific rates for the formation of perillyl acetate from glucose (light grey bars) by mixed-strain resting-cell suspensions composed of *E. coli* BL21 DE3 (pMVAidi, pTAC:AGPSS2:LS) and either *E. coli* MG1655 (pTAC:POH) (**A, B**) or *E. coli* MG1655 (pTAC:CymA) (**C, D**). The numbers on the x-axes refer to the applied cell dry weight (CDW) concentrations of *E. coli* BL21 (pMVAidi, pTAC:AGPSS2:LS), whereas the concentration of the MG1655 strains was 1 $g_{cdw}\,L^{-1}$ in all cases. Specific rates refer to the total CDW concentration (sum of both strains). Panels **B** and **D** represent the volumetric perillyl acetate formation rates for mixtures with CYP153A6 (**B**) or CymA (**D**). Means and error bars refer to two independent resting cell assays. One unit

(U) is defined as one µmol of product formed per minute. The units are either normalized to the total biomass concentration (U g_{cdw}^{-1}) or to the reaction volume (U L^{-1}).

Tables

Table I: List of *E. coli* strains and plasmids that were applied in this study.

Strain	Relevant characteristics	Reference
E. coli DH5α	F^- Φ80*lac*ZΔM15 Δ(*lac*ZYA-*arg*F) U169 *rec*A1 *end*A1 *hsd*R17 (rK^-, mK^+) *pho*A *sup*E44 λ_B^- *thi*-1 *gyr*A96 *rel*A1	(Hanahan 1983)
E. coli BL21 (DE3)	F_B^- *omp*T *hsd*SB(rB–, mB–) *gal dcm* λ(DE3 [lacI lacUV5-T7 gene 1 *ind*1 *sam*7 *nin*5])	(Studier and Moffatt 1986)
E. coli JM101	*gln*V44 *thi*-1 *sup*E Δ(lac-proAB) F'[$lacI^q$ lacZΔM15 traD36 $proAB^+$]	(Messing 1979)
E. coli MG1655	F^- λ^- ilvG- rfb-50 rph-1	(Bachmann 1987)
E. coli W3110	F^- λ^- rph-1 IN(rrnD–rrnE)1	(Bachmann 1972)
P. putida DSMZ12264	*Pseudomonas putida* GS1 wild-type	DSMZ
Plasmids		
pMVAidi	p15A, cm^R, P_{lac}, *ato*B-*erg*13-tHMGR1-*erg*12-*erg*8-*erg*19-*idi*1	(Willrodt et al. 2014)
pTAC:LS:AGPPS2	pMB1, amp^R, P_{tac}, $lacI^q$, truncated and codon-optimized LS and GPPS2 genes from *M. spicata* and *A. grandis*, respectively	(Willrodt et al. 2014)
pCom8:PFR1500	pMB1*, gm^R, P_{alkB}, *alkS*, genes encoding CYP153A6, FdR, and FdX from *Mycobacterium* sp. HXN1500	(van Beilen et al. 2005)
pCom8:PFR1500L	pCom8:PFR1500 with gene encoding AlkL from *P. putida* GPo1	(Cornelissen et al. 2013)
pTAlk:POH	pTAC:LS:AGPPS2 with P_{alkB}, *alkS*, and genes encoding CYP153A6, FdR, and FdX from *Mycobacterium* sp. HXN1500	this study

pTAC:POH	pTAC:LS:AGPPS2 with the CYP153A6 gene between the LS and GPPS2 genes and the FdX and FdR genes after the GPPS2 gene	this study
pTAC:POHf	pTAC:POH, translational fusion between LS and CYP153A6	this study
pTAC:CymA	pMB1, amp^R, P_{tac}, $lacI^q$, *cymAa* and *cymAb* genes from *P. putida* GS1	this study
pTAC:POH:CymA	pTAC:CymA with truncated and codon-optimized LS gene from *M. spicata*	this study

Table II: POHAc production performance of *E. coli* MG1655 (pTAC:POH, pMVAidi) in different reaction setups: two-liquid phase fermentation with growing cells (2-LP), the single-strain (RCA single) and the mixed-strain resting cell approach (RCA mixed). Means and standard deviations were retrieved from 2 (for 2-LP and RCA single) or 4 (for RCA mixed) independent experiments.

Parameter	**2-LP**[a]	**RCA single**	**RCA mixed**[b]
Volume/ mL_{aq}	80	25	25
concentration/ $mg_{POHAc}\ L_{aq}^{-1}$	6.8 ± 0.3	1.8 ± 0.3	21.7 ± 5.0
biomass concentration/ $g\ L_{aq}^{-1}$	1.1 ± 0.1	8.0 ± 0.0	11.0 ± 0.0
$Y_{p/x}$/ $mg_{POHAc}\ g_{cdw}^{-1}$	6.2 ± 0.4	0.22 ± 0.03	2.0 ± 0.4
$Y_{p/s}$/ $mg_{POHAc}\ g_{glucose}^{-1}$	0.68 ± 0.03	0.02 ± 0.0[c]	0.26 ± 0.06[c]
duration/ h	48	3	3
averaged productivity/ $mg\ L^{-1}\ h^{-1}$	≥0.21	0.60 ± 0.09	7.34 ± 1.68

[a]For comparability reasons, the POHAc concentrations for the 2-LP cultivation of *E. coli* MG1655 (pMVAidi, pTAC:POH) are given as total product amount per aqueous phase volume (although the product resided in the organic phase).

[b]Mixed-strain data were taken from the 10:1 (EC_{Lim}:EC_{CYP}) biomass ratio set-up (see text and Fig. 7**A, B**).

[c]For the comparison of the POHAc yields on glucose, the amount of glucose which was consumed during the preceding biomass formation was added to the amount of glucose that was consumed during the resting cell fermentation.

[d]The productivity for the batch culture was approximated by assuming ~32 h POHAc production (4 h of pre-induction phase and ~12 h of late stationary phase were substracted as being non-productive).

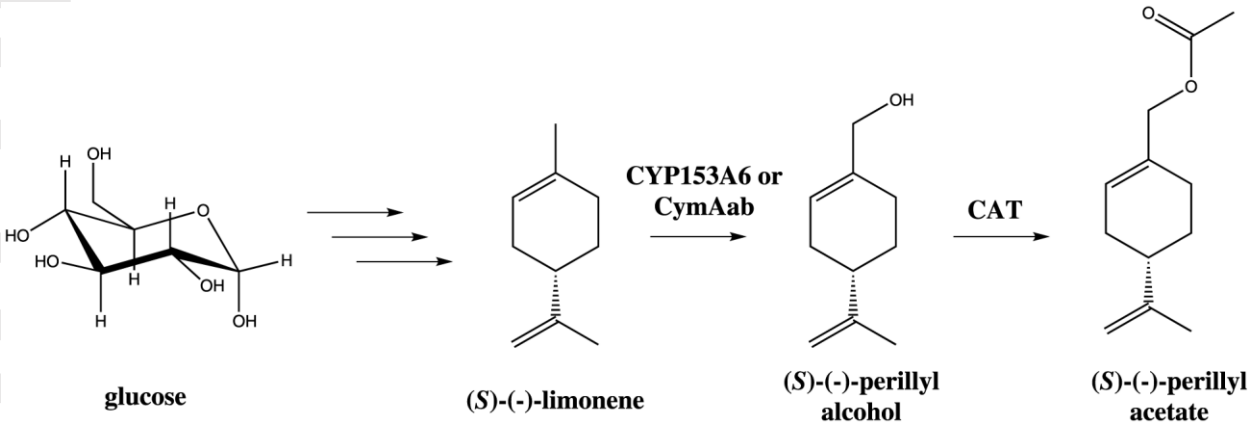

Figure 1

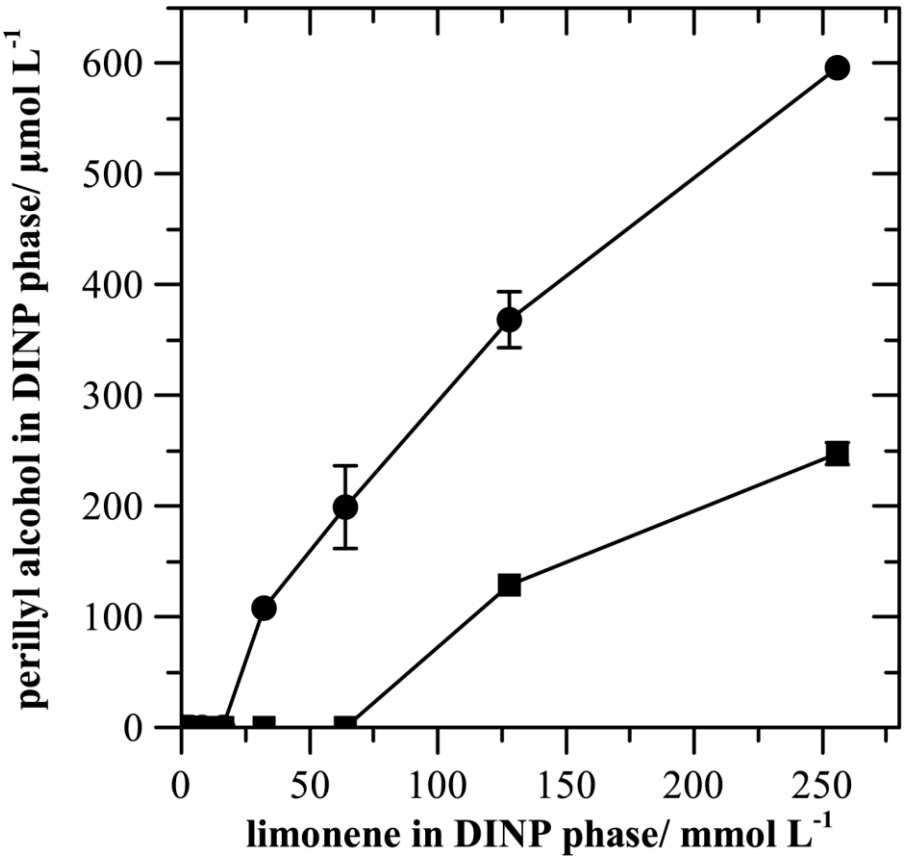

Figure 2

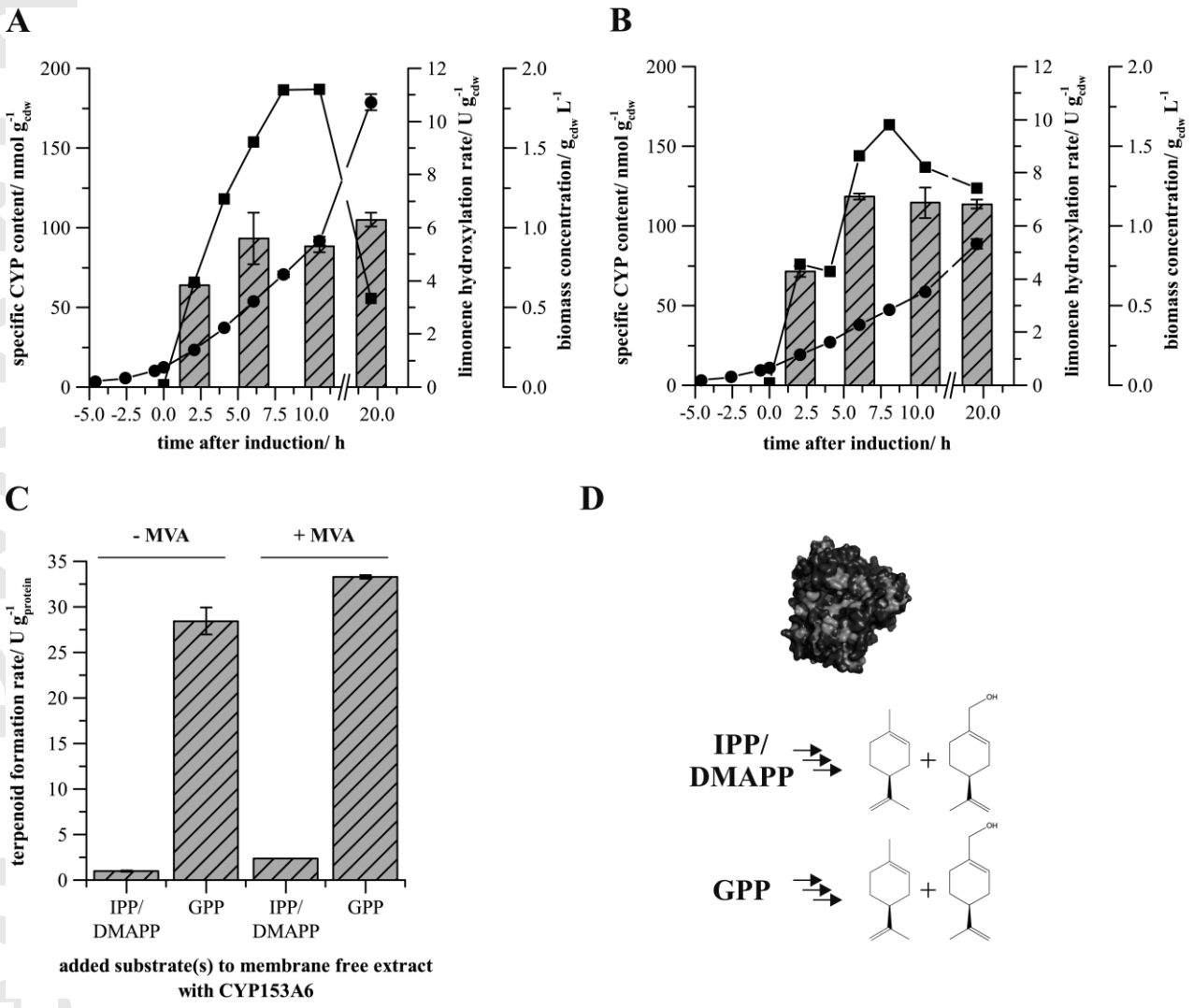

Figure 3

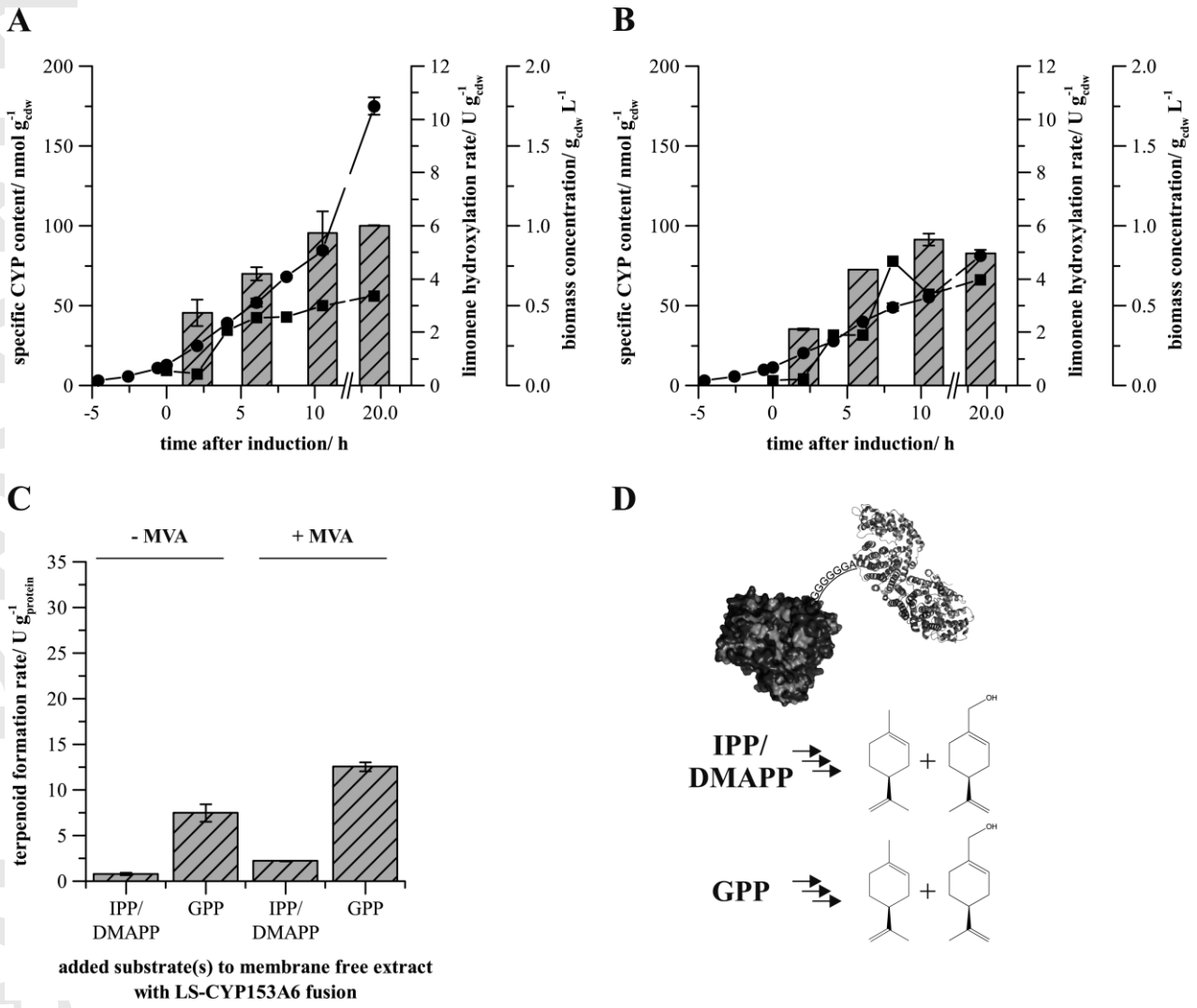

Figure 4

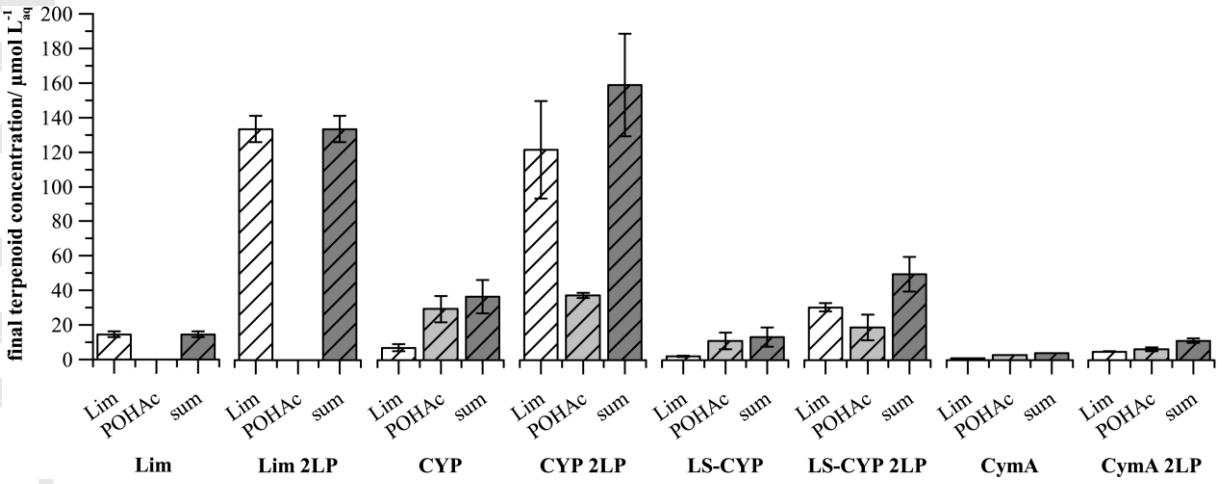

Figure 5

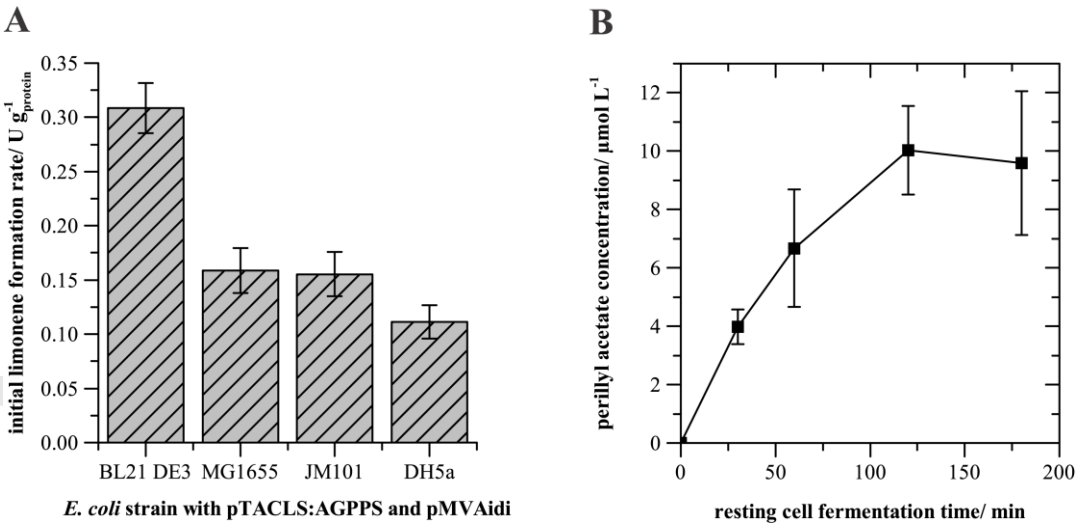

Figure 6

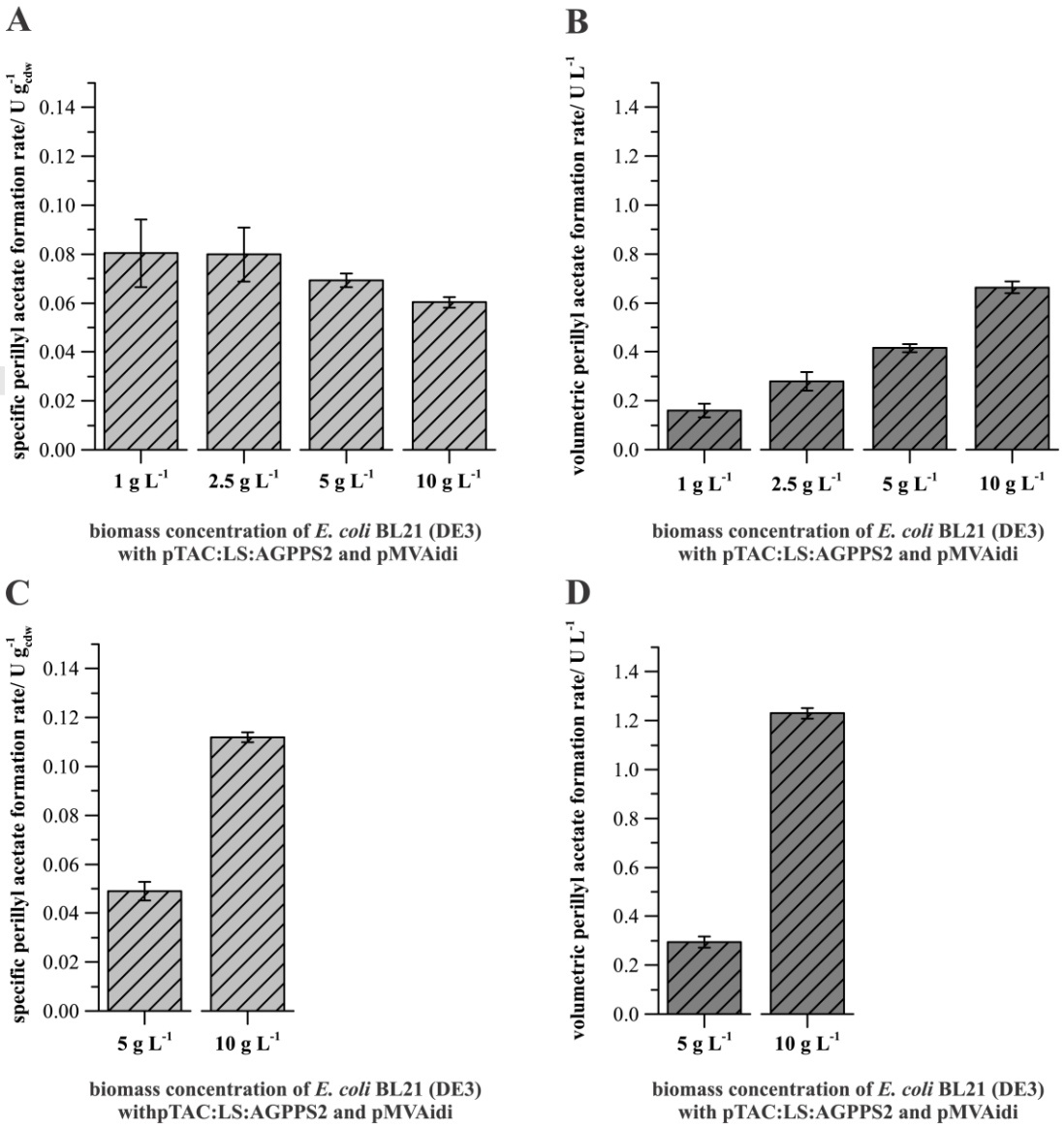

Figure 7